

PRESTACK SEISMIC DATA ENHANCEMENT WITH CRS PARAMETERS

M. Baykulov and D. Gajewski

email: *mikhail.baykulov@zmaw.de*

keywords: *Common Reflection Surface (CRS) stack, CRS supergather, partial CRS stacking*

ABSTRACT

Kinematic wavefield attributes or CRS parameters computed during the automatic CRS stack are used to enhance the quality of prestack seismic reflection data. Based on the CRS travelttime formula, partial stacked CRS supergatherers are computed. These gathers are regularized and have better signal to noise (SN) ratio compared to original CMP gathers. Improved prestack data could be used in any conventional processing tool (e.g., velocity analysis or prestack depth migration) instead of original data, providing enhanced images and better quality control.

Application of the new method to synthetic and real low-fold seismic data from a Jurassic salt plug in the area of the Glueckstadt Graben, Northern Germany, are presented. Significant improvement of the quality of seismic gathers as well as time and depth-migrated sections is a key result of the process.

INTRODUCTION

The quality of reflection seismic data is very important for seismic processing. It depends on a number of factors, e.g. the topography of the surface, the complexity of the subsurface, and the technical equipment used in the acquisition. The presence of natural and anthropogenic factors can affect land seismic measurements. Rivers and different topography structures as well as populated areas complicate the reflection data acquisition and lead to an irregular acquisition geometry resulting in regionally sparse data. Inhomogeneities in the subsurface, the presence of fault structures and strong velocity contrasts like in the areas of salt plugs lead to decreasing the SN ratio of the data. Quite often the quality of old seismic reflection data, which needs to be reprocessed, is comparably low, because of the short maximum offsets and low CMP fold. All these factors lead to a complicated and instable processing, e.g. by stacking velocity analysis and velocity model building. Therefore, the quality of time and depth migrated stacked sections is poor. The described shortcomings complicate a residual moveout analysis to update the velocity models. The CRS stack technology was already successfully applied to enhance the time and poststack depth migrated sections of old low-fold data from Northern Germany (see Yoon et al., 2007). It can also be used to improve the quality of prestack data. Based on the CRS travelttime formula, where the dip of the reflector element is incorporated, the SN ratio of the data can be significantly increased by applying of partial stack. Also the elimination of seismic data gaps in the areas of complex topography and the regularization of data can be improved with the partial stack technology.

THEORY

CRS travelttime

The CRS stack is a multi-parameter stacking technique. The travelttime t of reflection events is described by three parameters α , R_n and R_{nip} (see Eq. 1) instead of one parameter V_{nmo} for the classical CMP stack (Eq. 2) (see e.g. Mann, 2002; Mueller, 1999). In the following this parameter triplets are referred to as the

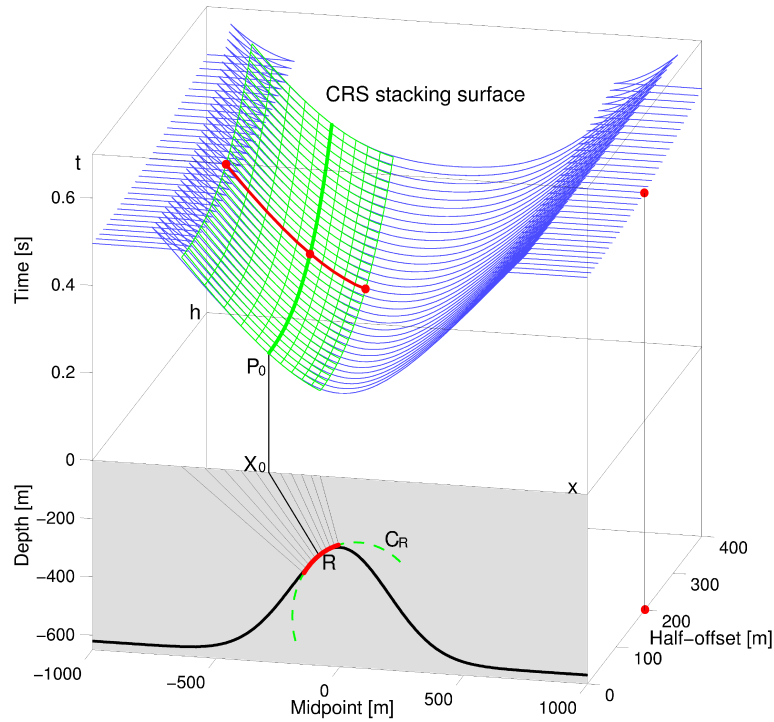


Figure 1: CRS stacking surface for a constant velocity medium modified after Mueller (1999). The CRS stack sums the data along the green surface and assigns the result to point P_0 . This stacking surface results from approximating the true subsurface reflector by a reflector segment that has locally the same curvature as the true reflector. Partial CRS stack performs the summation of data along the midpoint displacement coordinate (red line on the CRS stacking surface) and assigns the result to the certain offset in the supergather (in this example half-offset = 200 m).

CRS stacking parameters. In the equations h is half source-receiver offset, m is the midpoint displacement with respect to the considered CMP position and t_0 corresponds to the zero offset (ZO) two-way traveltimes (TWT). In Eq. 1 α is the angle of emergence of the ZO ray, V_0 is the near surface velocity, R_n and R_{nip} are radii of curvature of the normal (N) wave and normal-incidence-point (NIP) wave, respectively.

$$t^2[m, h] = \left(t_0 + \frac{2 \sin \alpha}{V_0} m \right)^2 + \frac{2 t_0 \cos^2 \alpha}{V_0} \left(\frac{m^2}{R_n} + \frac{h^2}{R_{nip}} \right) \quad (1)$$

$$t^2(h) = t_0^2 + \frac{4h^2}{V_{nmo}^2} \quad (2)$$

CRS supergatherers

The incorporation of the midpoint displacement into a partial CRS stack results in the construction of CRS supergather, where the dip of reflectors is included. Due to this the CRS supergather is superior to just merging several CMPs where the dip of the structure is not considered. Depending on the CMP displacement m , the CRS supergather contains a considerable larger number of traces than the CMP gather. The choice of the midpoint displacement m is important for the resulting lateral resolution of the following processing results. The size of the first projected Fresnel zone is a good guidance for this parameter which can be interpreted as the lateral extension of the supergather.

Assuming that the correct CRS stacking parameters are known for every time sample of the ZO section of the target zone, the prestack data can be summed up along the traveltimes surface defined by these

parameters to produce the partial stacked supergathers, where the dip of reflector elements is incorporated (see Fig. 1).

The red line on the CRS stacking surface (Fig. 1) corresponds to a reflection response at a certain half offset h . Summing the data along this line and assigning the result to the offset h yields a partial CRS stacked trace with better SN ratio. Repeating this for several offsets leads to a gather with higher fold than the original data. The better SN ratio is reached by stacking the data in the midpoint dimension. Higher fold is obtained by stacking the data along the traveltimes curves corresponding to every half source-receiver offset present in the data. In case of real data with irregular geometry, the gaps in the CMP data can be filled using the information from the neighboring CMP gathers within the projected Fresnel zone (green colour in Fig. 1). For data with regular geometry, e.g. synthetic or marine data, there are different sets of offsets in neighboring CMP gathers, depending on the geometry of the acquisition. Taking all the offsets from neighboring CMPs into account increases the number of traces in the CRS gathers.

Search strategy

During the partial CRS stack the summation of data along the stacking surface is performed for every CMP gather and for every sample $A(t, h)$, where t is two way traveltime (TWT), and h is half source-receiver offset (see Fig. 2 and Fig. 3). To stack the data along the traveltimes surface corresponding to the event A , we have to find the accurate t_0 time and corresponding CRS parameters (α, R_n, R_{nip}). To find the CRS parameters the search procedure is performed and the best fitting hyperbola for every event A is determined (Fig. 3). All t_0 traveltimes within the range $[0; t]$ and the CRS parameters corresponding to every t_0 are tested to determine the hyperbola. After time t'_0 which corresponds to the minimum deviation between the computed and the observed traveltime for sample A is found, the corrected t_0 time is computed using the CRS stacking parameters to best fit the traveltime of the element A . Since the t'_0 time can have only discrete values, the computed t_0 time may deviate slightly from the t'_0 .

Using the CRS parameters α and R_{nip} corresponding to the t'_0 , the corrected t_0 time is found by Eq. 3, which is derived from Eq. 1 after solving the quadratic equation with $m = 0$ and neglecting the negative solution of t_0 .

$$t_0 = -\frac{h^2 \cos^2 \alpha}{V_0 R_{nip}} + \sqrt{\left(\frac{h^2 \cos^2 \alpha}{V_0 R_{nip}}\right)^2 + t^2} \quad (3)$$

Substituting the t_0 time from Eq. 3 in Eq. 1 yields the traveltime formula for partial CRS stacking surface (Eq. 4), with the CRS parameters corresponding to t'_0 .

$$t^2[m, h] = \left(-\frac{h^2 \cos^2 \alpha}{V_0 R_{nip}} + \sqrt{\left(\frac{h^2 \cos^2 \alpha}{V_0 R_{nip}}\right)^2 + t^2} + \frac{2 \sin \alpha}{V_0} m \right)^2 + \frac{2 \cos^2 \alpha}{V_0} \left(-\frac{h^2 \cos^2 \alpha}{V_0 R_{nip}} + \sqrt{\left(\frac{h^2 \cos^2 \alpha}{V_0 R_{nip}}\right)^2 + t^2} \right) \left(\frac{m^2}{R_n} + \frac{h^2}{R_{nip}} \right) \quad (4)$$

Depending on the quality of data and the acquisition geometry, the optimal stacking apertures in both h and m directions must be chosen accordingly. This choice may be also influenced by the aim of processing. Although in most cases it is sufficient to stack along one certain half-offset h as it is shown in red colour in Fig. 1, the half-offset aperture can be extended for better regularization. In all examples in this paper the midpoint aperture was the same as used in the CRS stack, and half-offset aperture was set up to $[h - dh; h + dh]$, where dh is a half receiver interval.

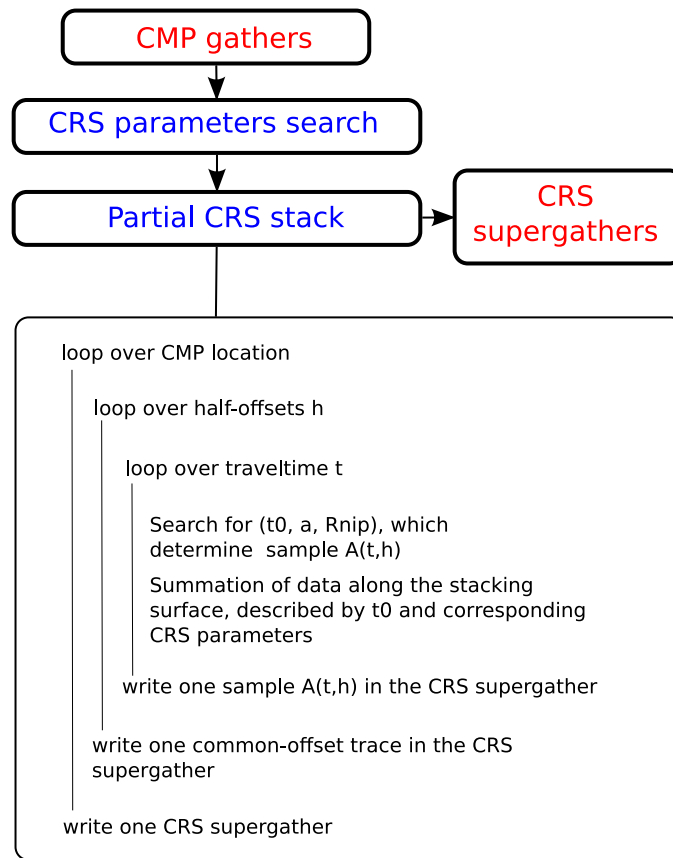


Figure 2: Workflow to obtain the CRS supergathers.

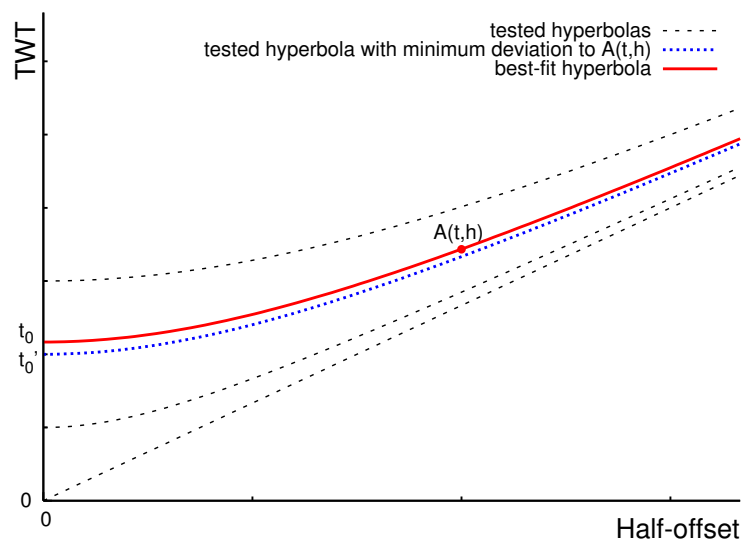


Figure 3: Tested traveltime curves to find the best-fit hyperbola for the sample $A(t, h)$ in the CRS supergather. The tic interval of the TWT axis corresponds to the time sample rate of the data.

RESULTS

In order to demonstrate the potential and advantages of partial CRS stack method, it is applied to the Sigsbee 2A synthetic dataset.

Noise free synthetic data

Sigsbee 2A is a constant density acoustic dataset released in 2001 by the "SMAART JV" consortium. The data do not contain free surface multiples and almost no internal multiples due to very low acoustic impedance contrasts. Sigsbee2A models the geologic setting found in on the Sigsbee escarpment in the deep water Gulf of Mexico. A number of normal and thrust faults are present in the data. The source interval was 45.72 m. 348 channels per shot were used with the receiver spacing of 22.86 m. Therefore the resulting CMP interval is 11.43 m, and maximum CMP fold is 87. The data were sampled every 8 ms with a total recording time of 12 s. In Fig. 4(a) the typical CMP gather up to 3500 m offset and TWT=10 s is shown.

500 CMP gathers were processed with the CRS stack method. The CRS parameters were used to compute the CRS supergathers. The midpoint aperture was set up to 260 m at TWT=2.3 s and 900 m at TWT=11 s and interpolated linearly for intermediate values. The offset range of 914 m at TWT=2.3 s and 3810 m at TWT=11s was used and again interpolated linearly. Half-offset aperture used by partial CRS stacks for every offset h was set up to $[h - 11.43m; h + 11.43m]$. The resulting CRS supergather is shown in Fig. 4(b).

The CRS supergather has 4 times more traces than the CMP gather shown in Fig. 4(a). Whereas only every fourth CMP gather has the same sets of source-receiver offsets, in every CRS supergather all these offsets are present. The CRS supergather is muted according to the defined offset range. Because of the larger number of traces, reflections in the CRS supergathers look sharper and could be better distinguished in comparison to the CMP gather.

CMP gathers and CRS supergathers were stacked with the same stacking velocities obtained by the automatic CMP stack. Resulting ZO sections are shown in Fig. 5. The ZO CMP stack section (Fig. 5(a)) displays a low quality in the areas of fault structures and strong dipping layers. CRS supergather stack (Fig. 5(b)) shows a better continuity of horizons at all time levels and produced better images of conflicting dip areas. The section is better suited for the interpretation than the CMP stack section.

Synthetic data with noise

To show the advantages of applying the CRS supergather method to noisy data, the direct waves were muted, and gaussian noise with SN=20 was added to the synthetic seismograms. As a result, only the strongest reflections like the water bottom (4 s TWT) and the bottom of the model (9 s TWT) are visible (Fig. 6(a)). Since the amplitudes of all other reflections are lower, they are almost not visible. After performing the CRS stack the obtained CRS parameters were used to build the supergathers. The result is shown in Fig. 6(b). Compared to the CMP gather the reflections in the CRS supergather are clearly visible at all times. Although there is still noise present, the SN ratio is significantly increased. The comparison of stacked CMP gathers and CRS supergathers (Fig. 7) demonstrates the advantage of CRS supergathers. Whereas the CMP stack of noisy seismograms (Fig. 7(a)) has lower SN ratio than the CMP stack of original data without noise (Fig. 5(a)), the stacked CRS supergathers (Fig. 7(b)) have almost no visible differences compared to the stacked supergathers without noise (Fig. 5(b)). Only in the water and in the areas of low reflectivity (8-9 s TWT, 0-100 CMP) the presence of noise is visible in Fig. 7(b). This means, that the CRS supergathers are very stable to the presence of non-coherent noise. This advantage, however, requires the accurate determination of CRS parameters (α , R_n , R_{nip}).

Real land data

The formation of CRS supergathers was also applied to real data from Northern Germany. A part of a seismic reflection profile located north of the river Elbe and crossing the Jurassic salt plug in the Glueckstadt Graben area was processed. The data were acquired in the 1980s. Explosive sources were used with an average shot spacing of 120 m. 120 channels with a receiver spacing of 40 m were used to generate each

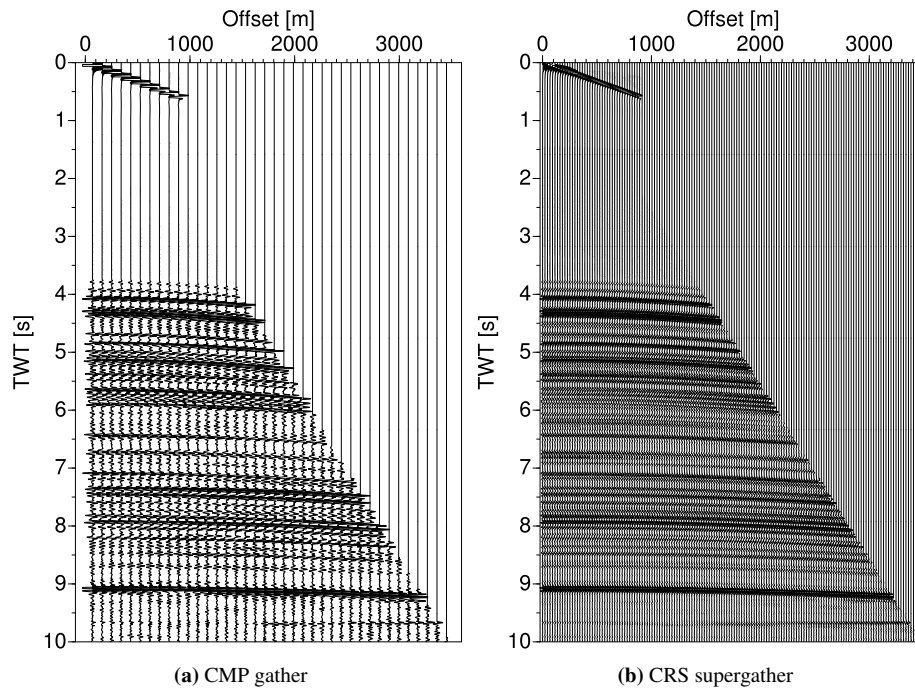


Figure 4: Noise free Sigsbee 2A data. Partially stacked CRS supergather (b) has 4 times as many traces as the original CMP gather (a), providing better images of reflection events.

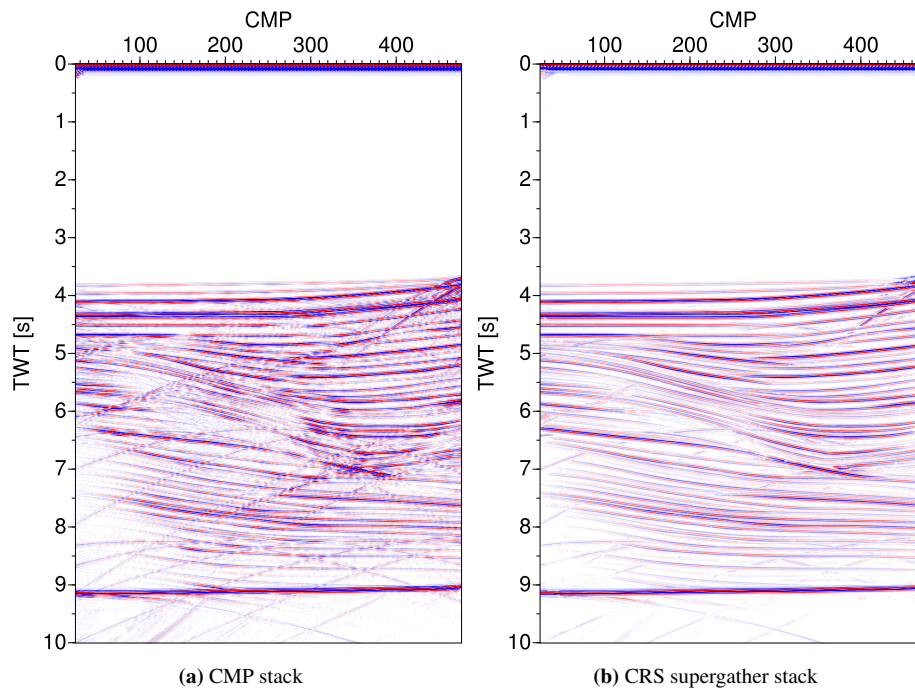


Figure 5: ZO time section of noise free stacked Sigsbee 2A data. Conventional CMP stack (a) has decreased quality in conflicting dips areas. CRS supergather stack shows better continuity of reflections and enhanced images of conflicting dip areas.

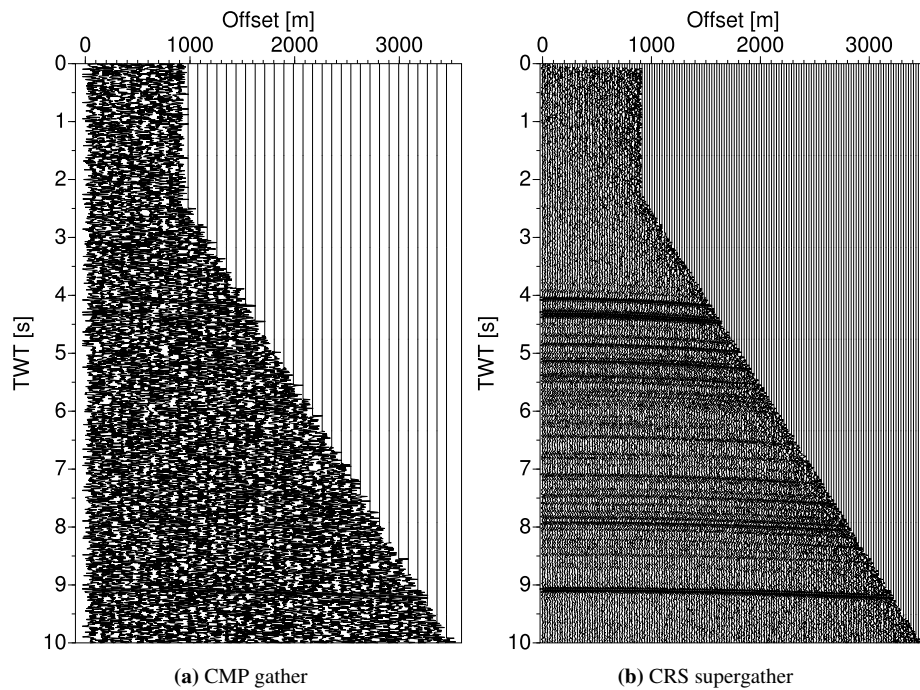


Figure 6: Sigsbee 2A data with noise. Reflections in the CMP gather (a) are hardly visible; CRS supergather (b) has significantly increased the SN ratio, and reflections are clearly visible at all times.

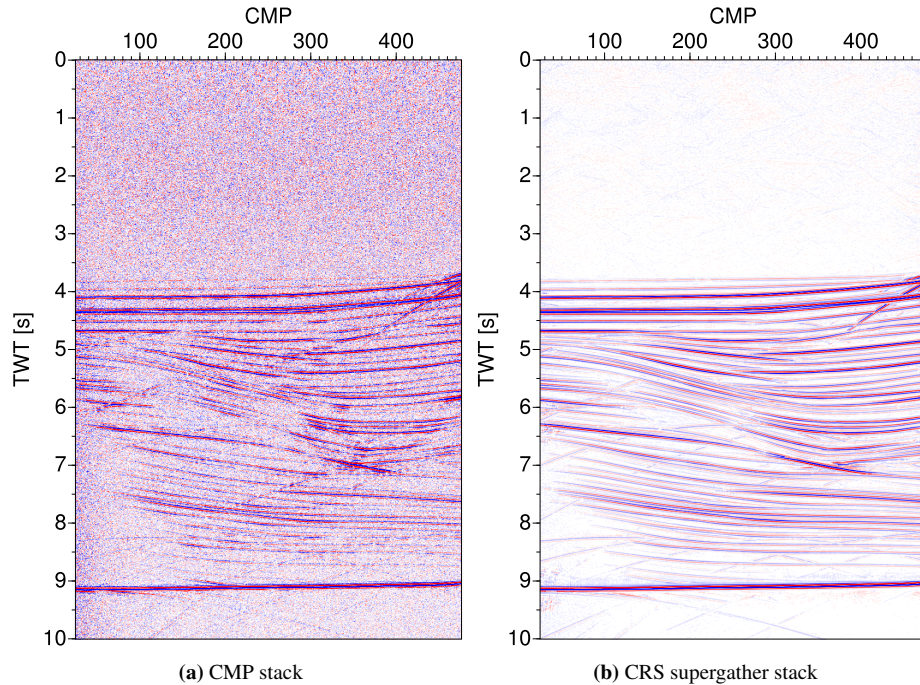


Figure 7: ZO time section of stacked Sigsbee 2A data with noise. The CMP stack has lower SN ratio compared to the CMP stack section without noise (Fig. 5(a)). The CRS supergather stack has almost no visual differences to the stacked section without noise (Fig. 5(b)); only in the water column and in low reflectivity areas (e.g. 8-9 s TWT, 25-100 CMP) the presence of noise is observed.

shot gather. Irregular shooting geometry leads to a varying CMP fold with an average of 20. A typical example of a preprocessed CMP gather is shown in Fig. 8(a). About 20 traces are located irregular over the full offset range. Irregularity of traces accompanied by the low SN ratio leads to difficulties in identifying reflections in the prestack data. Conventional binning of neighboring CMP gathers into a new gather also does not yield the desirable quality enhancement of the prestack data, because the merging of data without the correction or the dip of the layers leads to an energy smearing along these layers. Fig. 8(b) shows a binned gather obtained by combining 10 CMP gathers. The resulting CMP bin provided better coherency of the reflection elements in the upper part of the seismogram, but did not fill completely the gaps of data at certain offsets (around 2000 m and 3700 m). Combining more traces together as shown in Fig. 8(c) filled these gaps, but decreased the energy of reflection events. Performing a prestack depth migration (PreSDM) with these data yields a depth-migrated section with low SN ratio, which is rather difficult to interpret compared to poststack depth migrated section (for more details, please refer to the WIT-report "Revisiting the structural setting of the Glueckstadt Graben salt stock family, North German Basin" by Baykulov et al., 2007). Prestack depth migrated common-reflection-point (CRP) gathers are only partially suited for residual moveout analysis and control. Only the strongest reflectors at 2 km and 6 km depth can be seen in Fig. 9(a) and at 1.2 km depth in Fig. 9(c).

The automatic search of CRS parameters was performed and the partial stacked CRS supergathers were built. An example of CRS supergathers is shown in Fig. 8(d). A significantly larger number of traces is present in the CRS supergather compared to the original CMP gather. The traces are well distributed, filling the gaps visible in Fig. 8(a). Reflections are clearly visible at all times down to 4 s TWT. Also some events at TWT = 4.5-5 s, offset = 1000-2000 m are observed. Compared to the binned CMP gathers (Fig. 8(b), Fig. 8(c)), CRS supergather provide a better SN ratio and a better continuity of reflections at all time levels. Partially CRS stacked data can be used for any conventional processing, e.g., for more robust velocity analysis as well as for time and depth stacking and migration. Based on the depth migrated CRS supergathers residual moveout analysis and velocity model update can be performed.

Prestack Kirchhoff depth migration was applied to both sets of CMP gathers and CRS supergathers. The migration velocity model was obtained by the NIP-wave tomography inversion based on the CRS parameters (see also the WIT-report "Revisiting the structural setting of the Glueckstadt Graben salt stock family, North German Basin" by Baykulov et al., 2007). Because of the irregular geometry, the data were first preprocessed to build the binned common-offset gathers. Offset bin spacing of 100 m was used for both CMP gathers and CRS supergathers. Results of the PreSDM show a significantly improved depth migrated section using the CRS supergathers (compare Fig. 10 and Fig. 11). Horizons are more continuous, and a better SN ratio is obtained. PreSDM of CRS supergathers provided better depth migrated gathers compared to the original depth migrated CRP gathers (see Fig. 9). Reflectors are clearly visible and can be easily identified. The absence of residual moveouts in depth migrated CRS supergathers confirmed the accuracy of the velocity model used for migration that was hardly possible using the conventional CRP gathers.

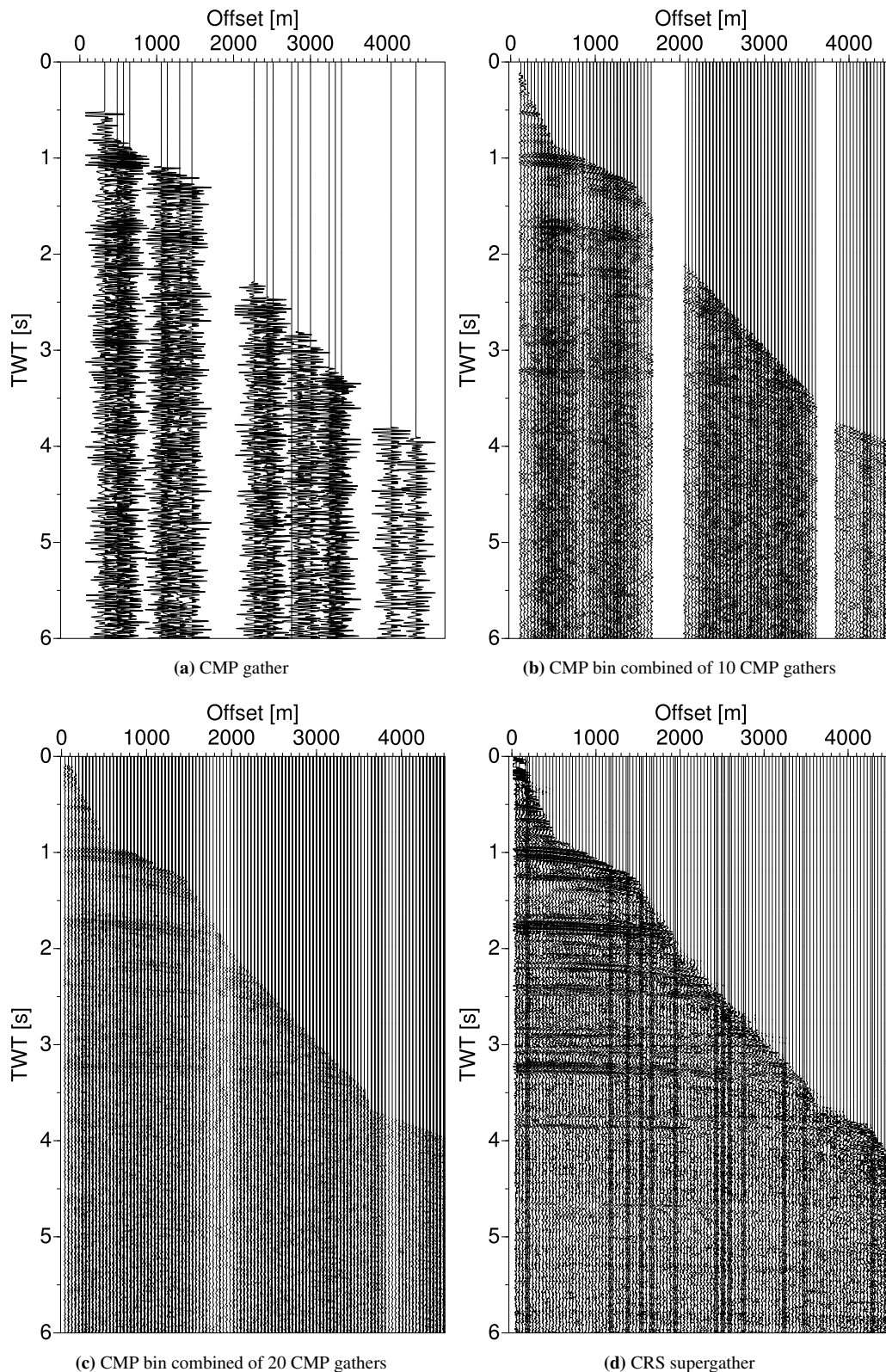


Figure 8: Real land data from Northern Germany. The CMP gather (a) has about 20 traces located irregularly and is not well suited for advanced seismic processing. No coherent reflection events can be observed. Combining more CMP gathers into a new one (b, c) increased the coherence of events, but do not increase the SN ratio. CRS supergathers provide an significantly increased SN ratio and increased reflection continuity, since the information about reflectors dips is incorporated in the partial stacks during the formation of supergathers.

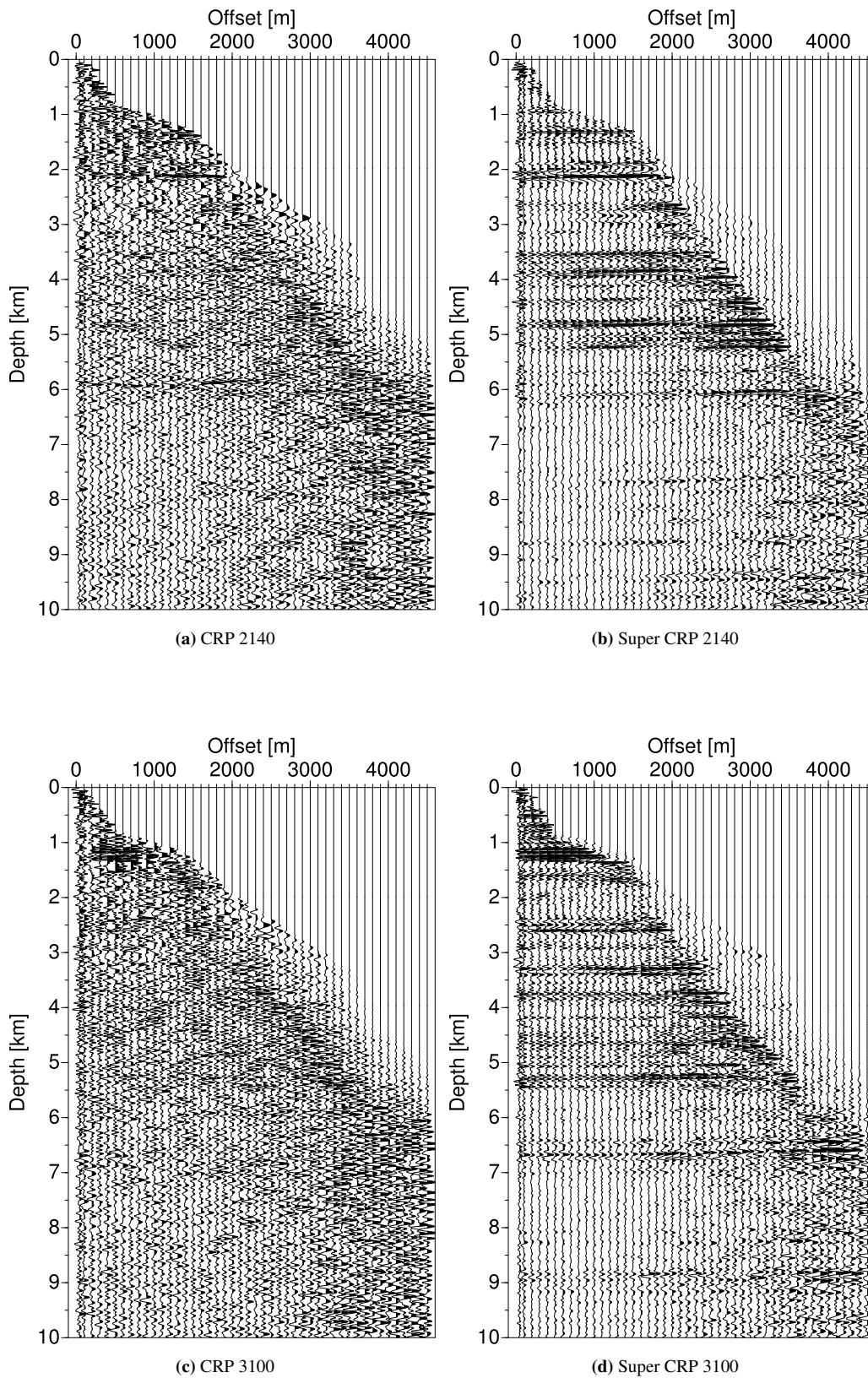


Figure 9: Prestack depth migrated CRP gathers located to the left and right of the salt plug (Fig. 10 and Fig. 11). Conventional CRP gathers display only the strongest reflectors at 2 km and 6 km depth for CRP 2140 (a) and at 1.2 km depth for CRP 3100 (c). The depth migrated CRS supergathers (b,d) have an increased SN ratio, and reflectors at the levels down to 9-10 km depth are visible.

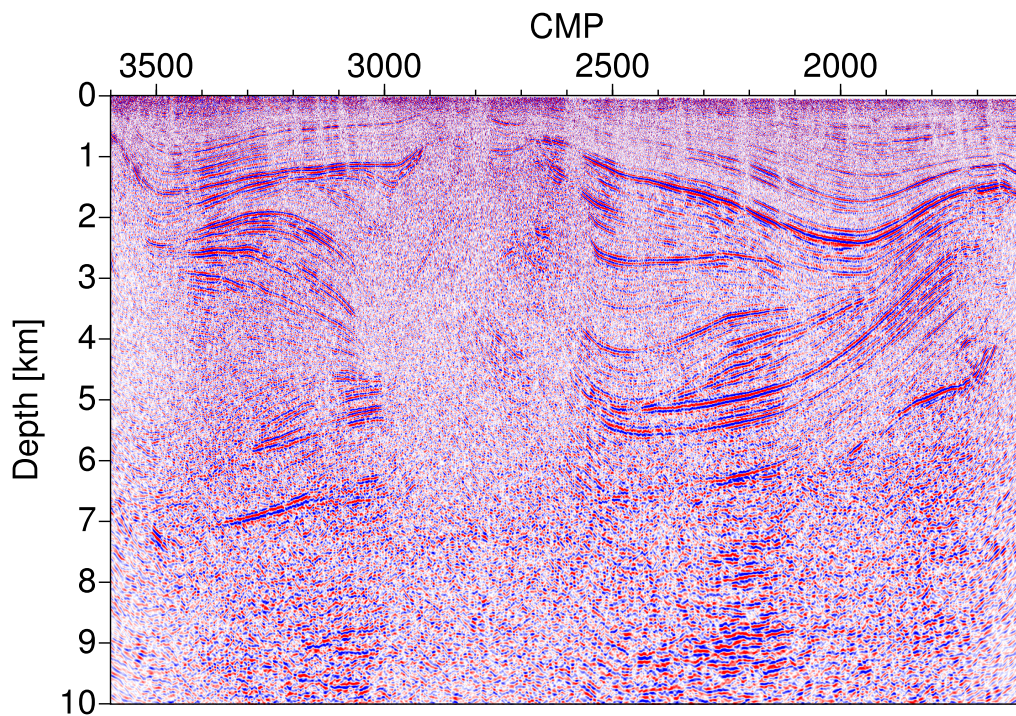


Figure 10: PreSDM of CMP gathers. SN ratio is low. Reflectors are not continuous, the internal structure of the salt plug and the reflectors below 7 km depth are hardly visible.

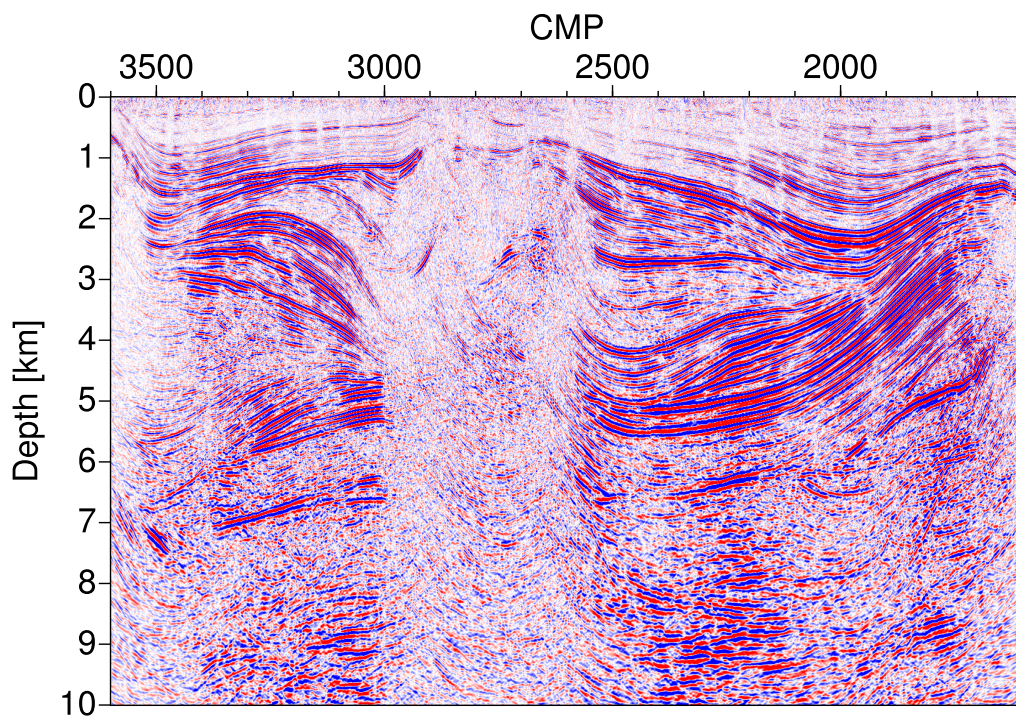


Figure 11: PreSDM of CRS supergathers. The image quality is significantly enhanced compared to Fig. 10. Horizons are more continuous, the enhanced SN ratio is obvious. Internal salt reflectors between 3000 and 2500 CMP at 2-6 km depth are identified. Also the image of the deeper part of the section below 7 km is improved.

CONCLUSION

The presented results of the partial CRS stack method have demonstrated the potential of this procedure to enhance the data quality and regularity. Despite the hyperbolic assumption of the method, the CRS supergathers are better regularized and have enhanced SN ratio than the low fold CMP gathers even in complex areas with presence of salt and strong dipping layers. The method was successfully implemented on synthetic data and on real land data from Northern Germany. The prestack depth migrated CRS supergathers allowed quality control of the velocity model used by migration, which was not possible by conventional processing. New depth migrated images provided an alternative view on the structural settings of the Glueckstadt Graben area, which is described in more details in the WIT-report "Revisiting the structural setting of the Glueckstadt Graben salt stock family, North German Basin" by Baykulov et al., 2007.

ACKNOWLEDGEMENTS

We are grateful to the Wave Inversion Technology (WIT) consortium for supporting this project. The synthetic seismic data were produced by the Subsalt Multiples Attenuation and Reduction Technology Joint Venture (SMAART JV). The real land data were kindly provided by the Wirtschaftsverband Erdöl- und Erdgasgewinnung (WEG) through the technical management of the German Society for Petroleum and Coal Science and Technology (DGMK). The processing of the data was partially supported through the grant Ga 350/12 of the priority program SPP 1135 of the German Research Foundation (DFG). We are thankful to Dr. Juergen Mann for the fruitful discussions and suggestions for modifying the 2D CRS code. Discussions with Stefan Duemmong are appreciated.

REFERENCES

- Mann, J. (2002). Extensions and Applications of the Common-Reflection-Surface Stack Method. *Logos Verlag Berlin. ISBN 3-8325-0008-1. PhD thesis, University of Karlsruhe, pages 2–52.*
- Mueller, T. (1999). The Common Reflection Surface Stack Method: Seismic Imaging without Knowledge of the Velocity Model. *Der Andere Verlag, Bad Iburg. ISBN 3-93436-606-6. PhD thesis, University of Karlsruhe, pages 9–36.*
- Yoon, M., Baykulov, M., Duemmong, S., Brink, H.-J., and Gajewski, D. (2007). Reprocessing of seismic reflection data with the common reflection surface (CRS) stack method: New insights into the crustal structure of Northern Germany. *Tectonophysics*, revised.